Supplementary information

Mst1 inhibits autophagy by promoting Beclin1-Bcl-2 interaction

Yasuhiro Maejima, Shiori Kyoi, Peiyong Zhai, Tong Liu, Hong Li,
Andreas Ivessa, Sebastiano Sciarretta, Dominic P. Del Re, Daniela K. Zablocki, Chiao-Po Hsu,
Dae-Sik Lim, Mitsuaki Isobe, and Junichi Sadoshima

Supplementary Figure 1-1

a

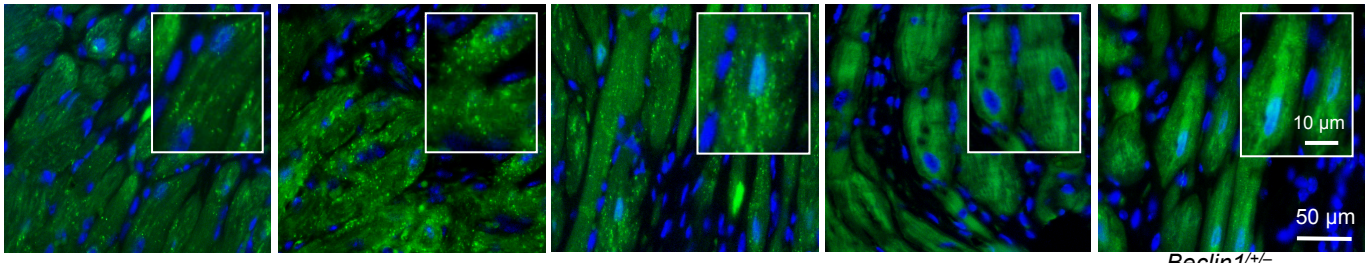

b

x Tg-GFP-LC3: 6W-MI

Sham	NTg	Tg-DN-Mst1	*Mst1*$^{-/-}$	*Beclin1*$^{+/-}$	*Beclin1*$^{+/-}$-Tg-DN-Mst1	6 week MI	NTg	Tg-DN-Mst1	*Mst1*$^{-/-}$	*Beclin1*$^{+/-}$	*Beclin1*$^{+/-}$-Tg-DN-Mst1
n	9	7	6	8	6	*N*	6	7	8	7	6
%FS (%)	37.11 ± 2.8	34.48 ± 3.83	34.11 ± 1.44	35.0 ± 2.1	37.06 ± 2.27	%FS (%)	17.13 ± 2.0	21.63 ± 0.8 *	21.43 ± 0.7 *	12.01 ± 1.21 *	12.05 ± 0.95 *
LVEF (%)	74 ± 2.6	71.19 ± 1.89	71.2 ± 1.9	71.94 ± 2.59	74.6 ± 2.7	LVEF (%)	42.59 ± 4.09	51.78 ± 3.98 *	51.41 ± 1.31 *	31.53 ± 2.77 *	32.05 ± 2.12 *
LVEDD (mm)	3.89 ± 0.12	3.48 ± 0.3	3.95 ± 0.24	3.53 ± 0.22	4.13 ± 0.22	LVEDD (mm)	6.01 ± 0.28	5.43 ± 0.17	4.82 ± 0.24 *	5.81 ± 0.99	5.59 ± 0.2
LVESD (mm)	2.45 ± 0.15	2.28 ± 0.21	2.61 ± 0.2	2.32 ± 0.21	2.62 ± 0.22	LVESD (mm)	4.96 ± 0.17	4.26 ± 0.16 *	3.78 ± 0.19 *	5.1 ± 0.32	4.86 ± 0.22
Lung/TL (mg/mm)	7.63 ± 0.34	7.85 ± 0.34	7.43 ± 0.18	7.25 ± 0.48	7.83 ± 0.58	Lung/TL (mg/mm)	11.63 ± 0.45	9.99 ± 0.69	9.78 ± 0.99	13.53 ± 0.34 *	13.51 ± 0.47 *

c

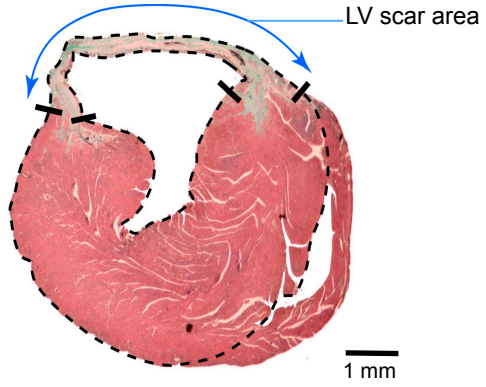

d

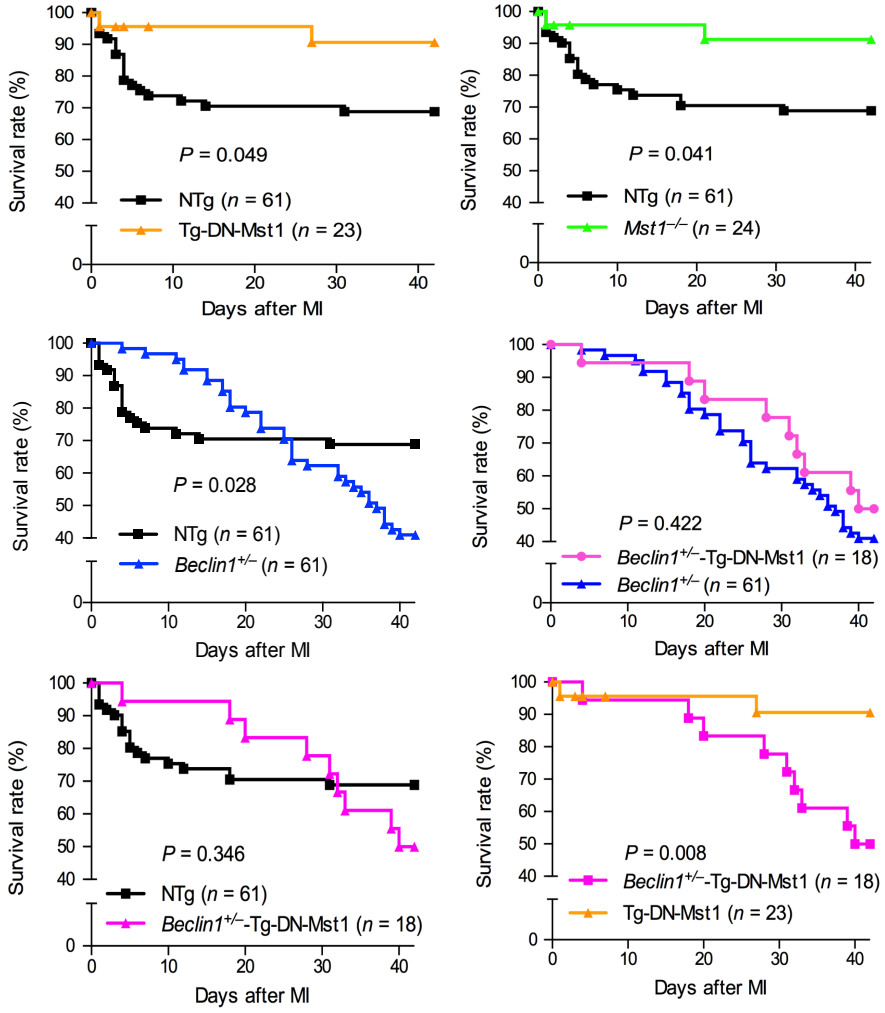

Supplementary Figure 1. Mst1 negatively regulates autophagy in the post MI heart, thereby promoting cardiac dysfunction through facilitating accumulation of protein aggresomes and p62/SQSTM1 in cardiomyocytes.
a, Representative images of GFP-LC3 puncta 6 weeks after coronary artery ligation in Tg-DN-Mst1, *Mst1*$^{-/-}$, *Beclin1*$^{+/-}$, *Beclin1*$^{+/-}$-Tg-DN-Mst1, and NTg mice that were crossed with Tg-GFP-LC3 mice are shown. Results represent means from 6 independent experiments. **b,** Echocardiographic analyses and postmortem lung weight measurements of Tg-DN-Mst1, *Mst1*$^{-/-}$, *Beclin1*$^{+/-}$, *Beclin1*$^{+/-}$-Tg-DN-Mst1, and NTg mice 6 weeks after coronary artery ligation or sham operation are shown. %FS: Fractional shortening, LVEF: LV ejection fraction, LVEDD: LV end-diastolic diameter, LVESD: LV end-systolic diameter, TL: Tibia length. Data are reported as mean ± SEM. * $P < 0.05$ vs NTg mice. **c,** Representative image of scar area of LV is shown. Scar area of LV evaluated by Masson's trichrome after 6 weeks of MI. **d,** Survival Tg-DN-Mst1, *Mst1*$^{-/-}$, *Beclin1*$^{+/-}$, *Beclin1*$^{+/-}$-Tg-DN-Mst1, and NTg mice was followed up for 6 weeks after coronary artery ligation. Kaplan-Meier analyses were used to compare the two groups. *P* values of the Log-rank (Mentel-Cox) test are presented.

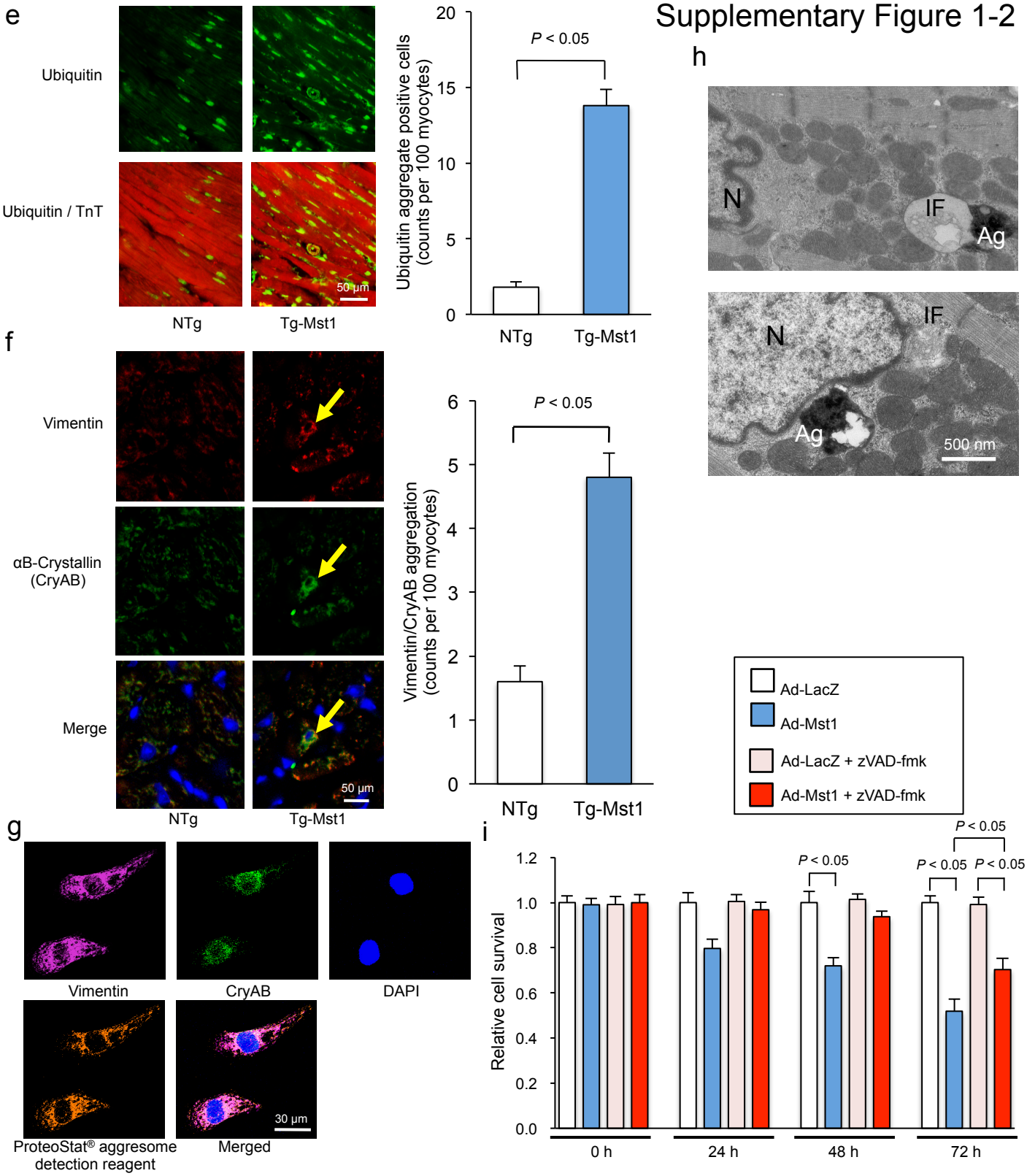

Supplementary Figure 1. (continued)

e, *Left:* Representative immunofluorescent images of staining with ubiquitin (green) and Troponin T (TnT, red) in NTg and Tg-Mst1 hearts are shown. *Right:* The number of ubiquitin aggregation-positive myocytes, indicated by yellow color in the merged images, was counted (n = 5 in each group). Data are reported as mean ± SEM. **f,** *Left:* Representative immunofluorescent images of staining with vimentin (red), αB-crystallin (CryAB, green), and DAPI (blue) in NTg and Tg-Mst1 mice are shown. *Right:* The number of CMs with vimentin colocalized with CryAB, indicated by yellow color (arrow), was counted (n = 5 in each group). Data are reported as mean ± SEM. **g,** Representative immunofluorescent images of staining with vimentin antibody labeled with Alexa Fluor® 647 (violet), CryAB antibody labeled with Alexa Fluor® 488 (green), DAPI (blue) and ProteoStat® aggresome detection reagent (555 nm, orange) in Ad-Mst1-transduced cardiomyocytes are shown. Results represent means from 4 independent experiments. **h,** Representative images of aggresomes detected by transmission electron microscopy in Tg-Mst1 hearts. The aggresomes (Ag), embedded in a dense meshwork of intermediate filaments (IF) adjacent to the Golgi apparatus (Go), appeared as electron dense amorphous structural objects. N: Nucleus. Results represent means from 4 independent experiments. **i,** Cell viability was evaluated in CMs after transduction with Ad-Mst1 or Ad-LacZ in the presence or absence of zVAD-fmk (100 μM), a pan-caspase inhibitor (n = 12 in each group). Data are reported as mean ± SEM.

Supplementary Figure 2-1

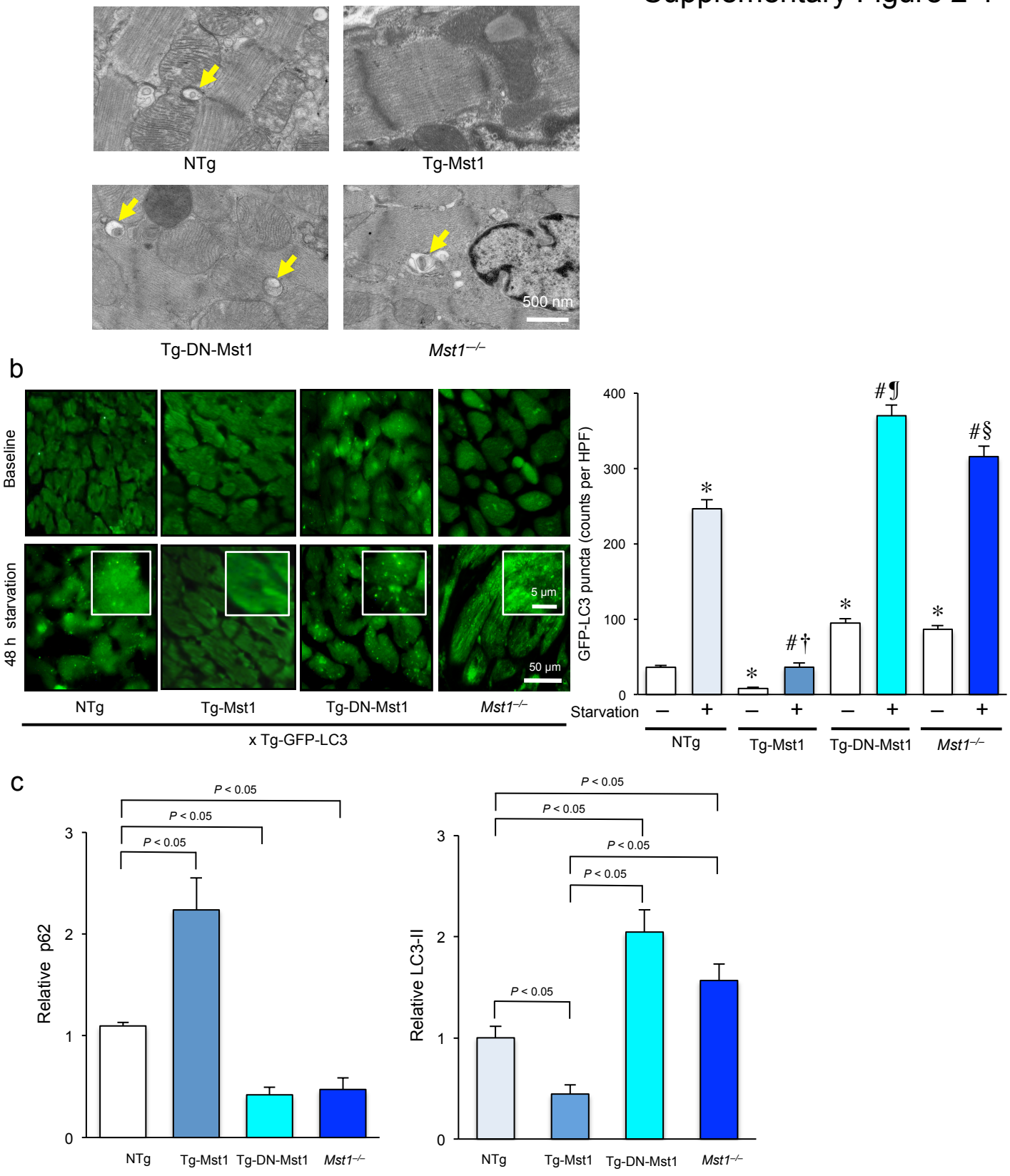

Supplementary Figure 2. Mst1 inhibits autophagy.
a, Representative images of autophagosomes (arrows) detected by transmission electron microscopy at baseline in Tg-Mst1, Tg-DN-Mst, *Mst1*$^{-/-}$, and NTg hearts are shown. Results represent means from 4 independent experiments. **b,** *Left:* Representative images of GFP-LC3 puncta at baseline and after 48 hours of starvation in Tg-GFP-LC3, Tg-Mst1-GFP-LC3, Tg-DN-Mst1-GFP-LC3 and *Mst1*$^{-/-}$-Tg-GFP-LC3 hearts are shown. Magnification of GFP-LC3 puncta is shown in the insets. *Right:* Quantitative analysis of the number of GFP-LC3 puncta is shown (n = 5 in each group). Data are reported as mean ± SEM. * $P < 0.05$ vs NTg - Baseline; # $P < 0.05$ vs NTg - starvation; † $P < 0.05$ vs Tg-Mst1 - Baseline; ¶ $P < 0.05$ vs Tg-DN-Mst1 - Baseline; § $P < 0.05$ vs *Mst1*$^{-/-}$ - Baseline. **c,** Quantitative analysis of the p62/SQSTM1 protein and LC3-II amounts in the immunoblot analyses of heart homogenates presented in Figure 2g is shown (n = 3 in each group). Data are reported as mean ± SEM.

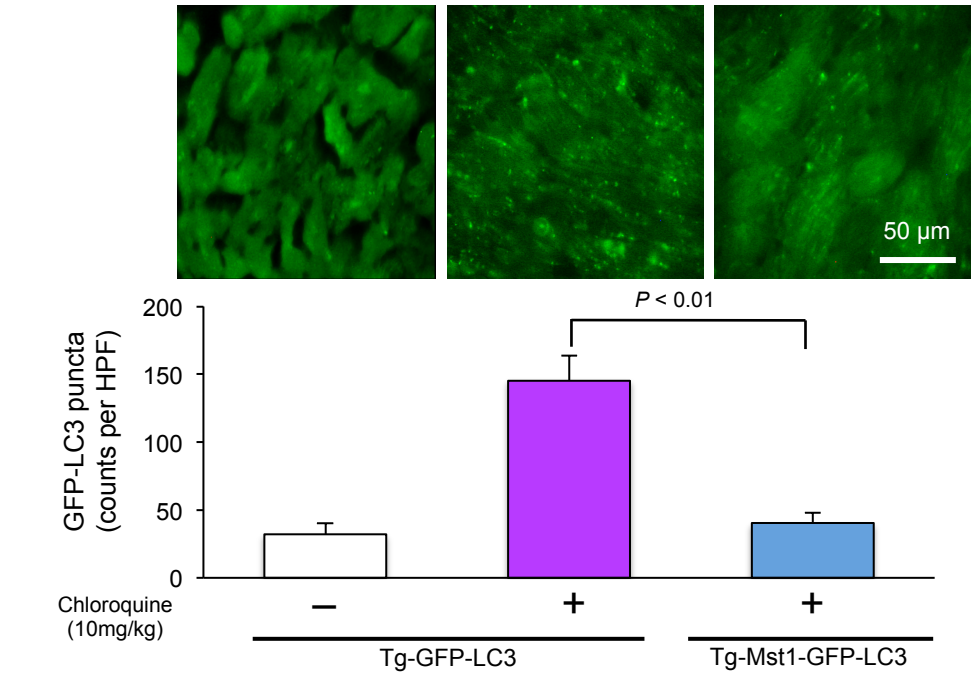

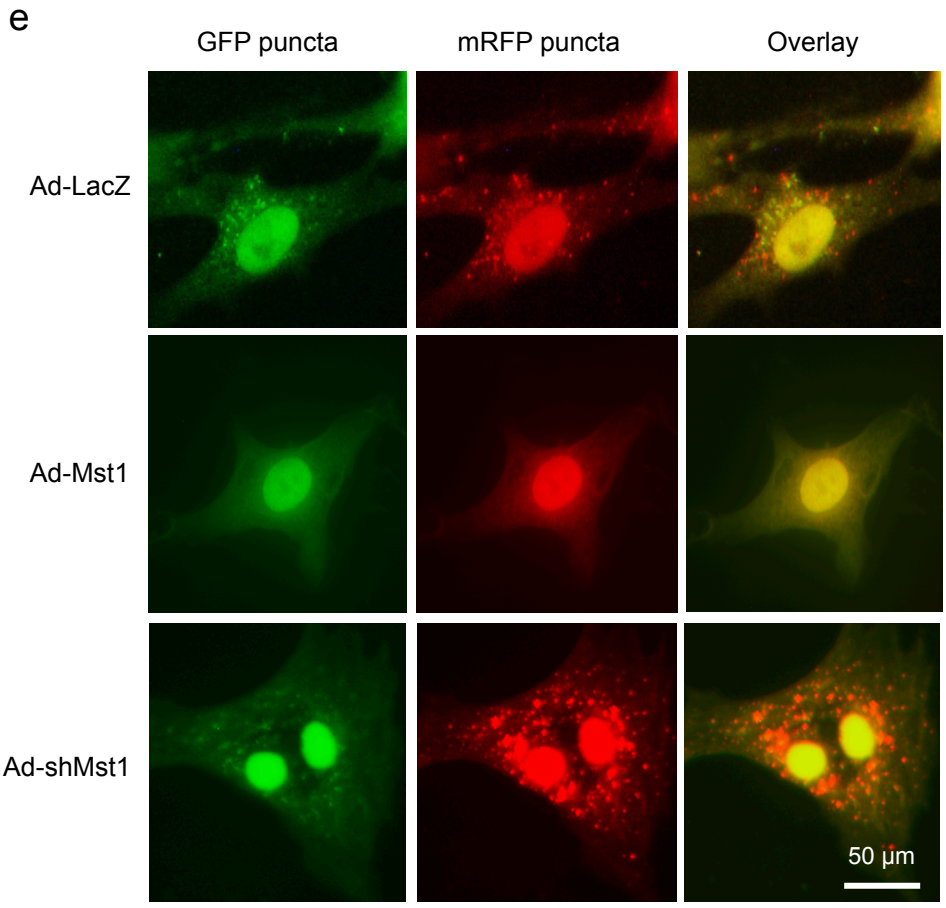

Supplementary Figure 2. (continued)
d, Tg-GFP-LC3 mice and Tg-Mst1-GFP-LC3 mice were treated with chloroquine (10mg/kg, i.p.) and evaluated 4 hours after injection. *Upper:* Representative images of GFP-LC3 puncta are shown. *Lower:* Quantitative analysis of the number of GFP-LC3 puncta is shown ($n = 4$ in each group). Data are reported as mean ± SEM. **e,** Cardiomyocytes were transduced with Ad-Mst1, Ad-shMst1, or Ad-LacZ 24 hours after Ad-mRFP-GFP-LC3 transduction and treated with glucose-free media. Representative images of fluorescent LC3 puncta. Quantitative analysis of the mean numbers of autophagosomes, represented by yellow puncta in merged images, and autolysosomes, represented by red puncta in merged images, per cell is shown in Figure 2h. Results represent means from 3 independent experiments.

Supplementary Figure 2-3

f

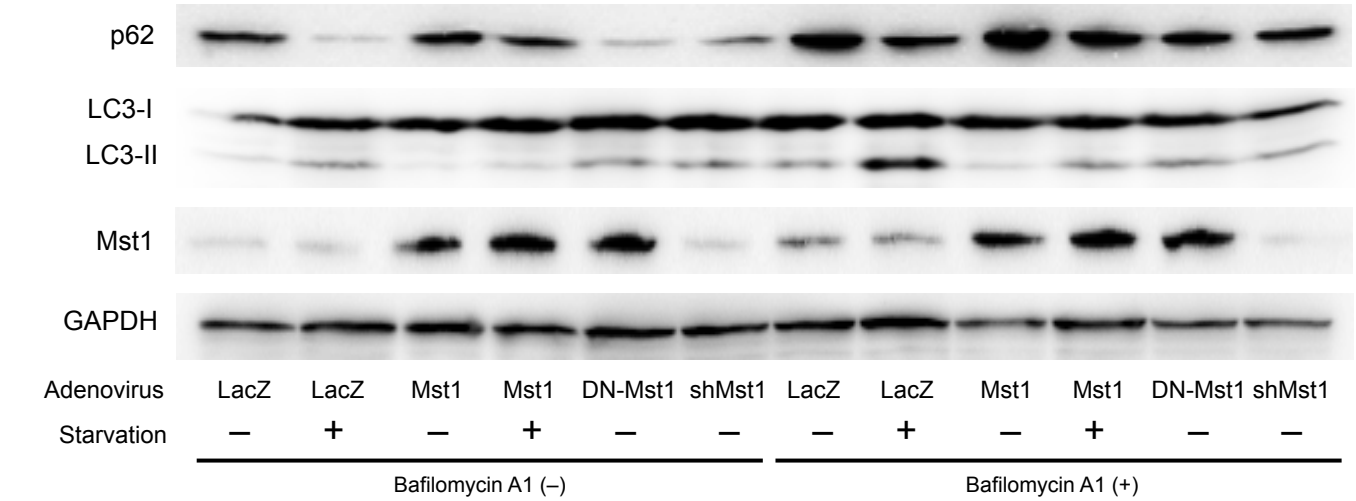

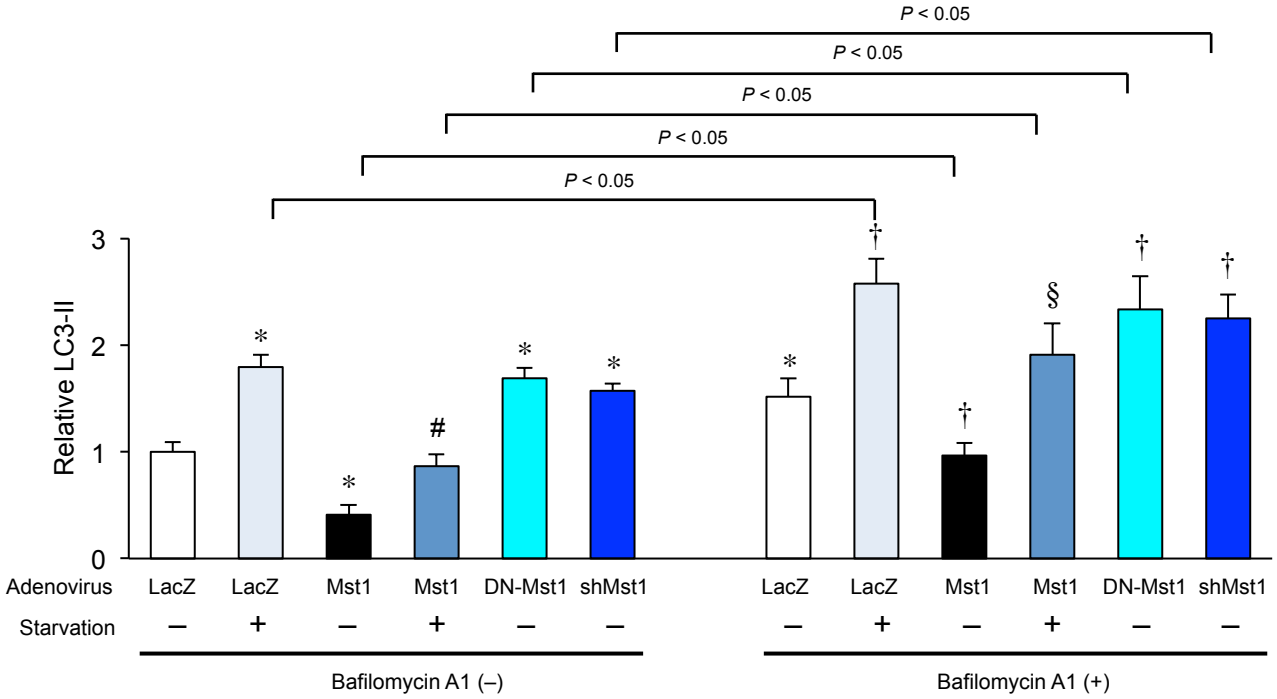

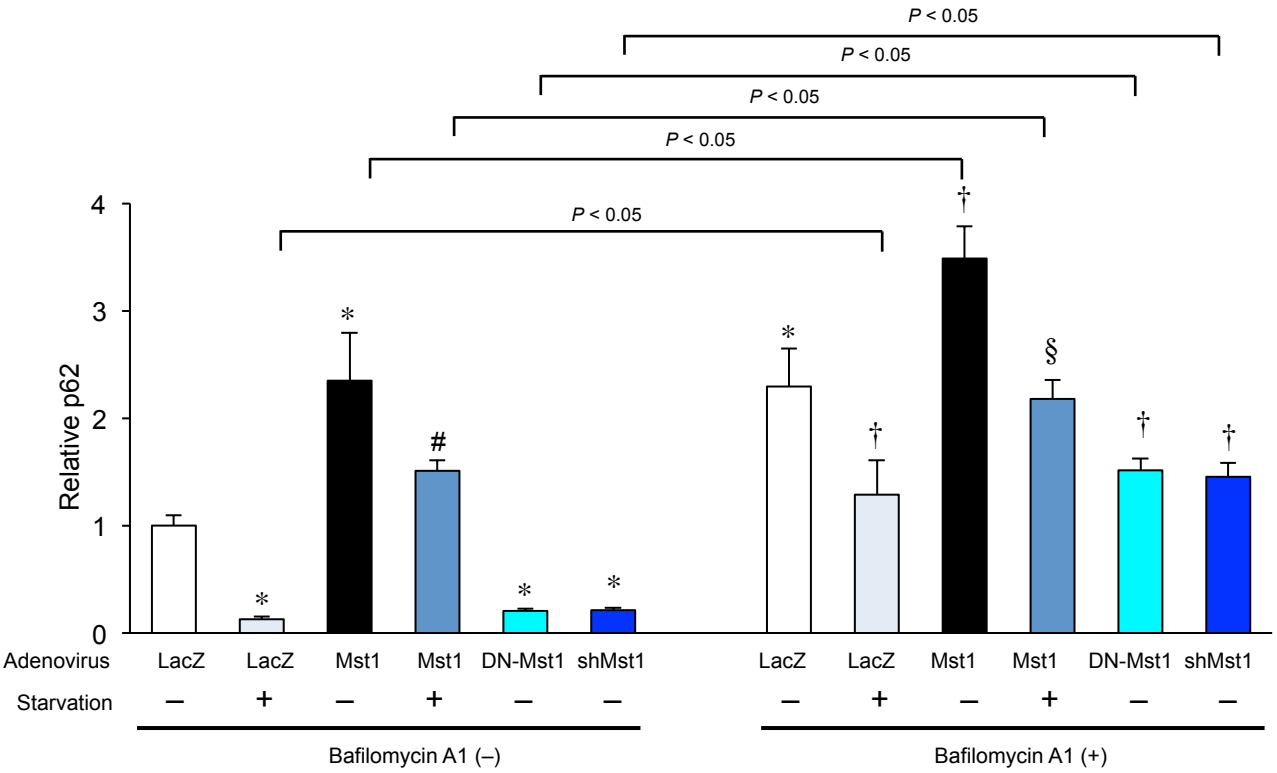

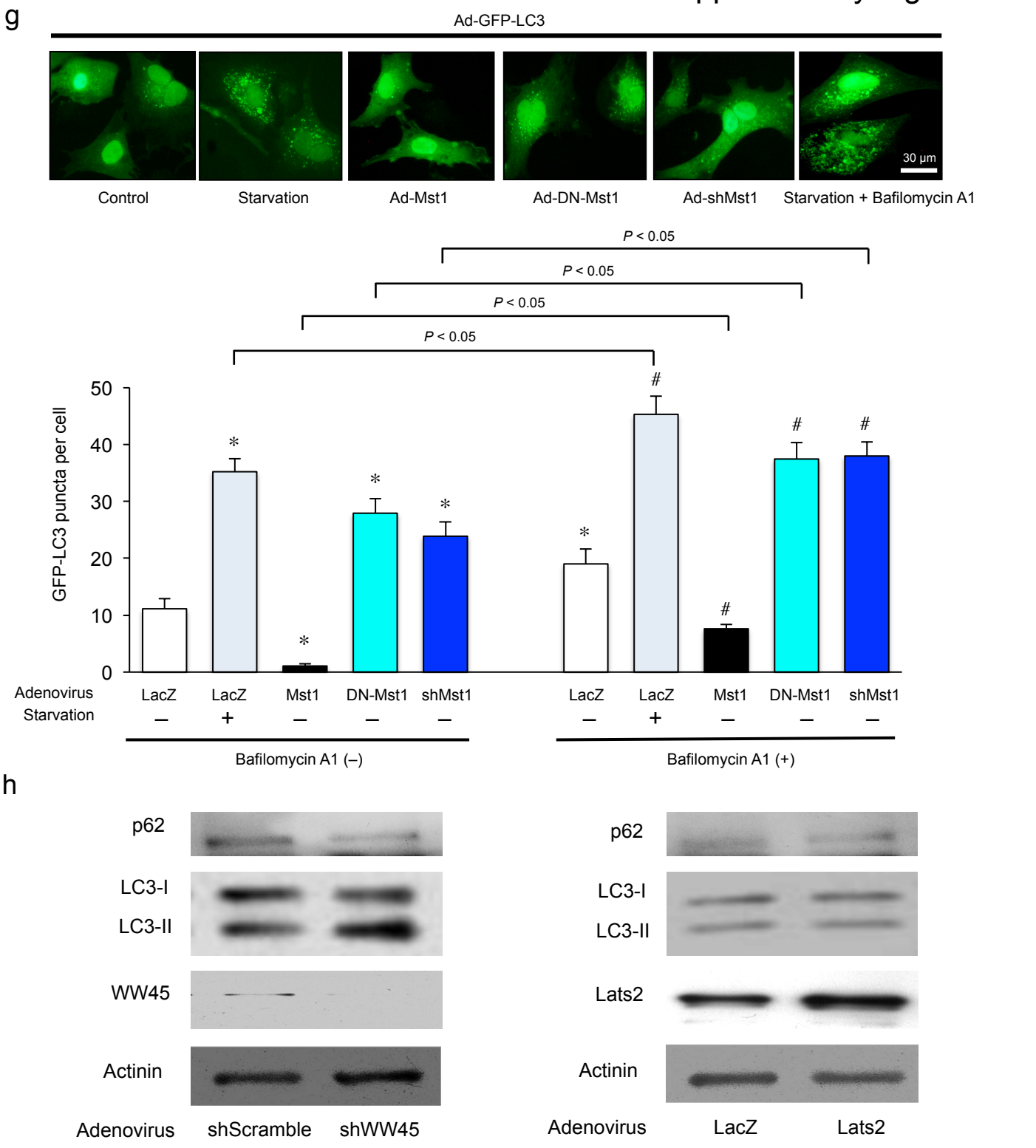

Supplementary Figure 2. (continued)
f, Cardiomyocytes transduced with Ad-Mst1, Ad-DN-Mst1, Ad-sh-Mst1 or Ad-LacZ were treated with a glucose-free medium for 4 hours. Some experiments were conducted in the presence of bafilomycin A1, a lysosomal inhibitor. *Upper:* Representative immunoblot pictures are shown. *Middle and Lower:* Quantitative analyses of the LC3-II and p62/SQSTM1 protein amounts are shown ($n = 3$ in each group). Data are reported as mean ± SEM. * $P < 0.05$ vs Ad-LacZ/GD(–)/Bafilomycin A1(–); # $P < 0.05$ vs Ad-LacZ/GD(+)/Bafilomycin A1(–); † $P < 0.05$ vs Ad-LacZ/GD(–)/Bafilomycin A1(+); § $P < 0.05$ vs Ad-LacZ/GD(+)/Bafilomycin A1(+). **g,** Cardiomyocytes were transduced with Ad-Mst1, Ad-DN-Mst1 or Ad-sh-Mst1 24 hours after Ad-GFP-LC3 transduction. *Upper:* Representative images of GFP-LC3 puncta are shown. *Lower:* Quantitative analysis of the number of GFP-LC3 puncta is shown ($n = 3$ in each group). Data are reported as mean ± SEM. * $P < 0.05$ vs Ad-LacZ/GD(–)/Bafilomycin A1(–); # $P < 0.05$ vs Ad-LacZ/GD(–)/Bafilomycin A1(+). **h,** Cardiomyocytes transduced with Ad-shWW45, Ad-Lats2, Ad-shScramble or Ad-LacZ were treated with a glucose-free medium for 4 hours. Representative immunoblot pictures are shown. Results represent means from 3 independent experiments.

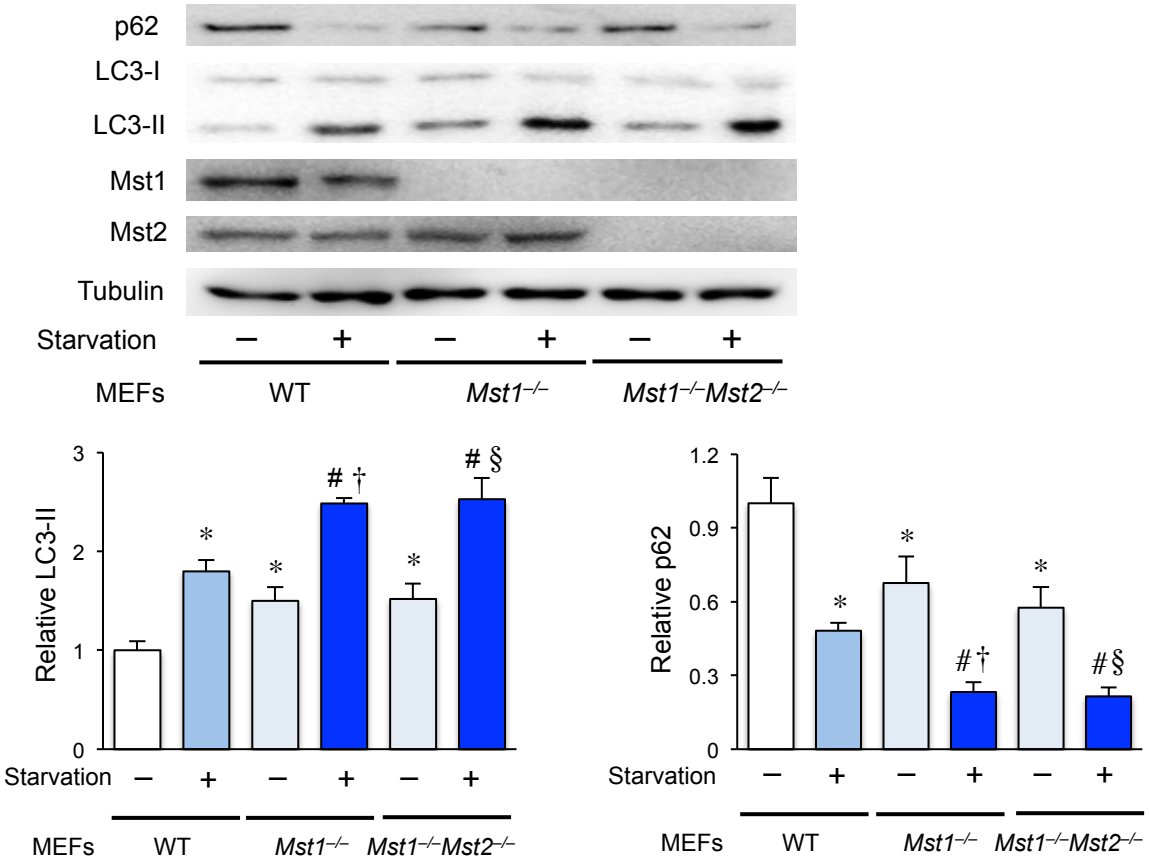

j

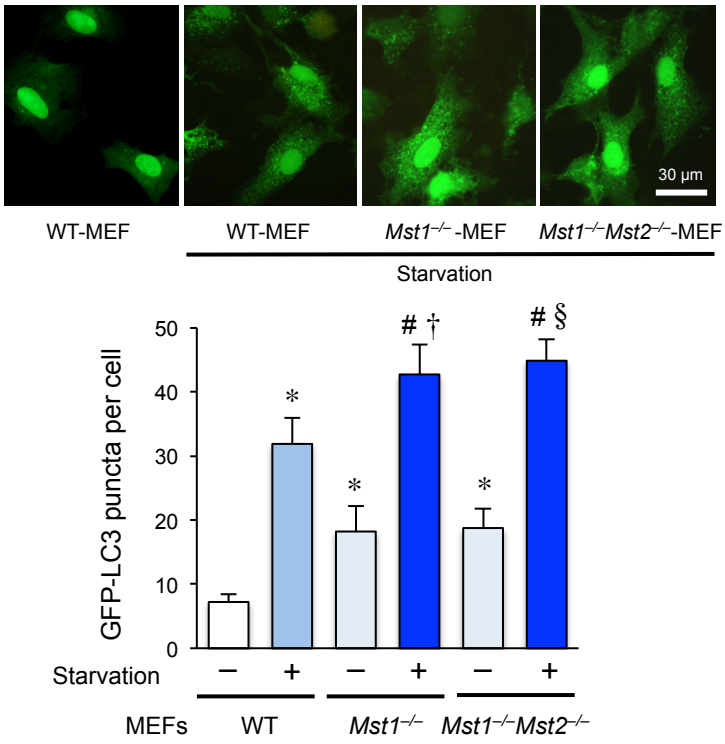

Supplementary Figure 2. (continued)
i, *Mst1*$^{-/-}$-MEFs, *Mst1*$^{-/-}$*Mst2*$^{-/-}$-MEFs, or WT-MEFs were treated with a glucose-free medium for 2 hours. *Upper:* Representative immunoblot pictures are shown. *Lower:* Quantitative analyses of the LC3-II and p62/SQSTM1 protein amounts are shown ($n = 3$ in each group). Data are reported as mean ± SEM. * $P < 0.05$ vs WT-MEFs/GD(–); # $P < 0.05$ vs WT-MEFs/GD(+); † $P < 0.05$ vs *Mst1*$^{-/-}$-MEFs/GD(-); § $P < 0.05$ vs *Mst1*$^{-/-}$*Mst2*$^{-/-}$-MEFs/GD(–). **j,** *Mst1*$^{-/-}$-MEFs, *Mst1*$^{-/-}$*Mst2*$^{-/-}$-MEFs, or WT-MEFs were transduced with Ad-GFP-LC3. *Upper:* Representative images of GFP-LC3 puncta are shown. *Lower:* Quantitative analysis of the number of GFP-LC3 puncta is shown ($n = 3$ in each group). Data are reported as mean ± SEM. * $P < 0.05$ vs WT-MEFs/GD(–); # $P < 0.05$ vs WT-MEFs/GD(+); † $P < 0.05$ vs *Mst1*$^{-/-}$-MEFs/GD(–); § $P < 0.05$ vs *Mst1*$^{-/-}$*Mst2*$^{-/-}$-MEFs/GD(–).

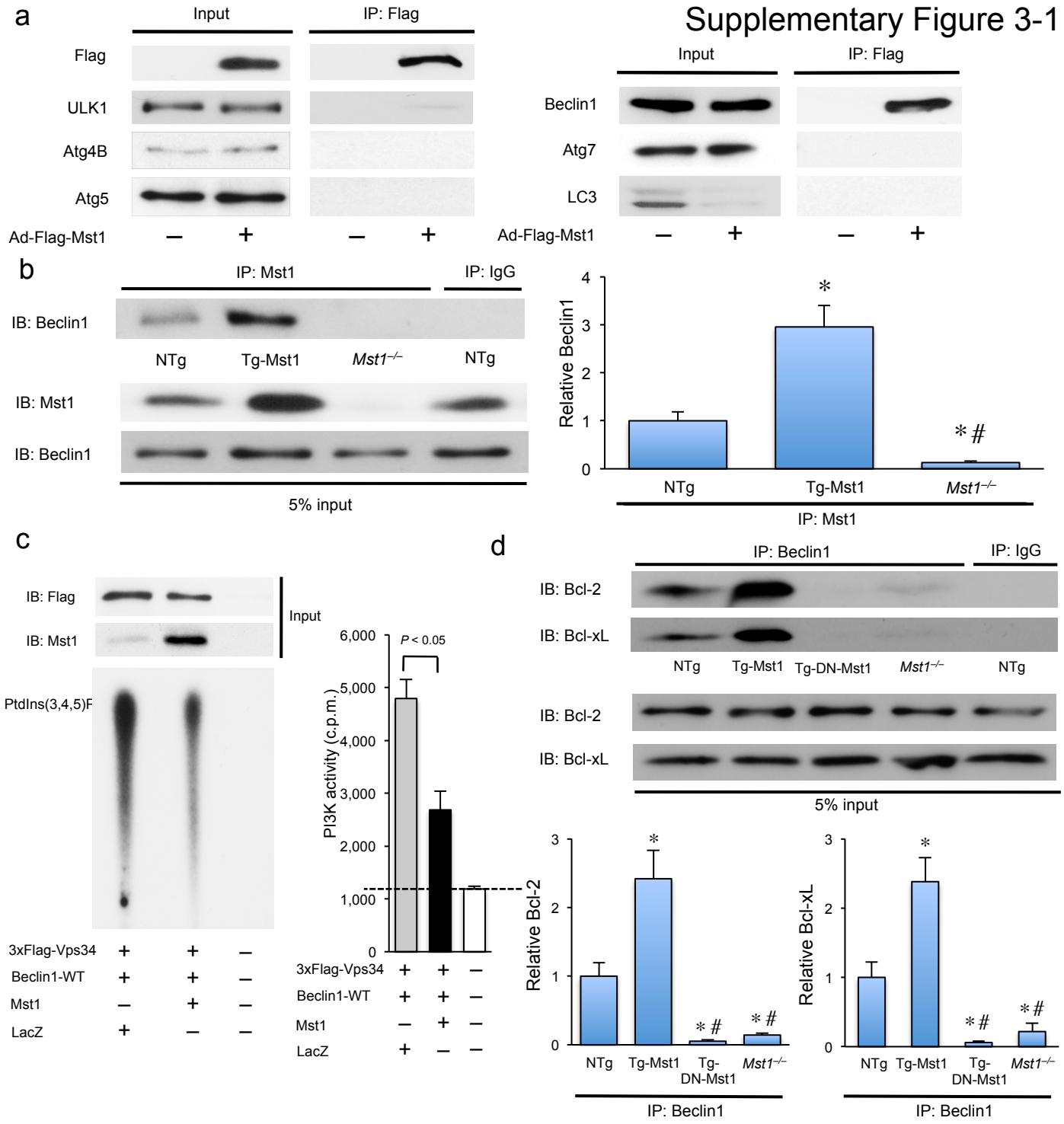

Supplementary Figure 3. Mst1 physically interacts with Beclin1 and enhances Beclin1 binding with Bcl-2/Bcl-xL, thereby inhibiting the kinase activity of the Beclin1-Vps34 complex.

a, Cardiomyocytes were transduced with or without Ad-3xFlag-Mst1. Forty-eight hours after transduction, lysates were extracted for co-immunoprecipitation (Co-IP) with Flag antibody, followed by probing with ULK1, Atg4B, Atg5, Beclin1, Atg7, LC3, or Flag antibodies. Representative images are shown. Results represent means from 3 independent experiments. **b,** Heart homogenates obtained from NTg, Tg-Mst1, or *Mst1*$^{-/-}$ mice were immunoprecipitated with covalently immobilized Mst1 antibody or control IgG with protein A/G agarose beads, followed by probing with Beclin1 antibody. *Left:* Representative images are shown. *Right:* Quantitative analysis of the Co-IP assays is shown (n = 5 in each group). Data are reported as mean ± SEM. * P < 0.05 vs NTg; # P < 0.05 vs Tg-Mst1. **c,** Cardiomyocytes were co-transduced with Ad-3xFlag-Vps34 and Ad-Beclin1-WT either in the absence or presence of Ad-Mst1. *Left:* Ad-3xFlag-Vps34 was immunoprecipitated with Flag antibody for the *in vitro* kinase assay. The resulting radioactive PtdIns(3,4,5)P_3 was separated by TLC. *Right:* Radioactive PtdIns(3,4,5)P_3 was excised from thin layer plates and the radioactivity was measured in an LSC (n = 4 in each group). Data are reported as mean ± SEM. **d,** Heart homogenates obtained from NTg, Tg-Mst1, Tg-DN-Mst1, or *Mst1*$^{-/-}$ mice were immunoprecipitated with covalently immobilized Beclin1 antibody or control IgG with protein A/G agarose beads, followed by probing with Bcl-2 or Bcl-xL antibodies. *Upper:* Representative images are shown. *Lower:* Quantitative analyses of the Co-IP assays are shown (n = 5 in each group). Data are reported as mean ± SEM. * P < 0.05 vs NTg; # P < 0.05 vs Tg-Mst1.

Supplementary Figure 3-2

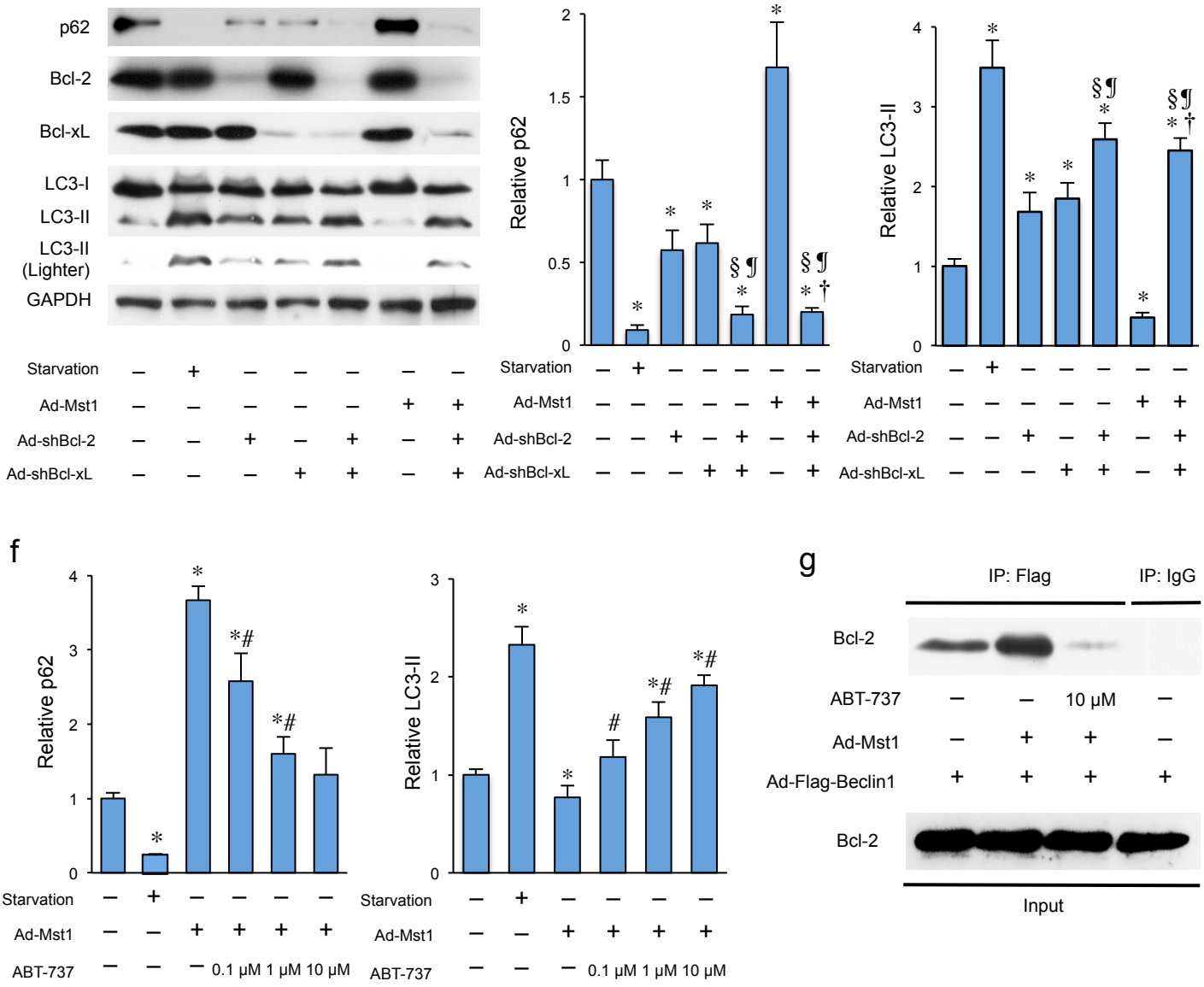

Supplementary Figure 3. (continued)

e, Cardiomyocytes were transduced with or without Ad-Mst1 either in the absence or presence of Ad-sh-Bcl-2 or Ad-sh-Bcl-xL. A sample from cardiomyocytes treated with glucose-free medium served as a positive control. *Left:* Representative immunoblots with p62/SQSTM1, Bcl-2, Bcl-xL, LC3 and GAPDH antibodies are shown. *Middle and Right:* Quantitative analyses of the p62/SQSTM1 protein and LC3-II amounts in the immunoblot analyses are shown ($n = 3$ in each group). Data are reported as mean ± SEM. * $P < 0.05$ vs untreated control; † $P < 0.05$ vs Ad-Mst1; § $P < 0.05$ vs Ad-shBcl-2; ¶ $P < 0.05$ vs Ad-shBcl-xL. **f,** Cardiomyocytes transduced with or without Ad-Mst1 were treated with ABT-737 (0, 0.1, 1, 10 μM) for 12 hours. Quantitative analysis of the p62/SQSTM1 protein and LC3-II amounts in the immunoblot analyses presented in Figure 3g is shown ($n = 3$ in each group). Data are reported as mean ± SEM. * $P < 0.05$ vs untreated control; # $P < 0.05$ vs Ad-Mst1. **g,** Cardiomyocytes transduced with Ad-3xFlag-Beclin1 either in the absence or presence of Ad-Mst1 were treated with or without 10 μM ABT-737. Forty eight hours after transduction, lysates were extracted for immunoprecipitation with Flag antibody or control IgG, followed by probing with Bcl-2 antibody. Representative images are shown. Results represent means from 3 independent experiments.

Supplementary Figure 4-1

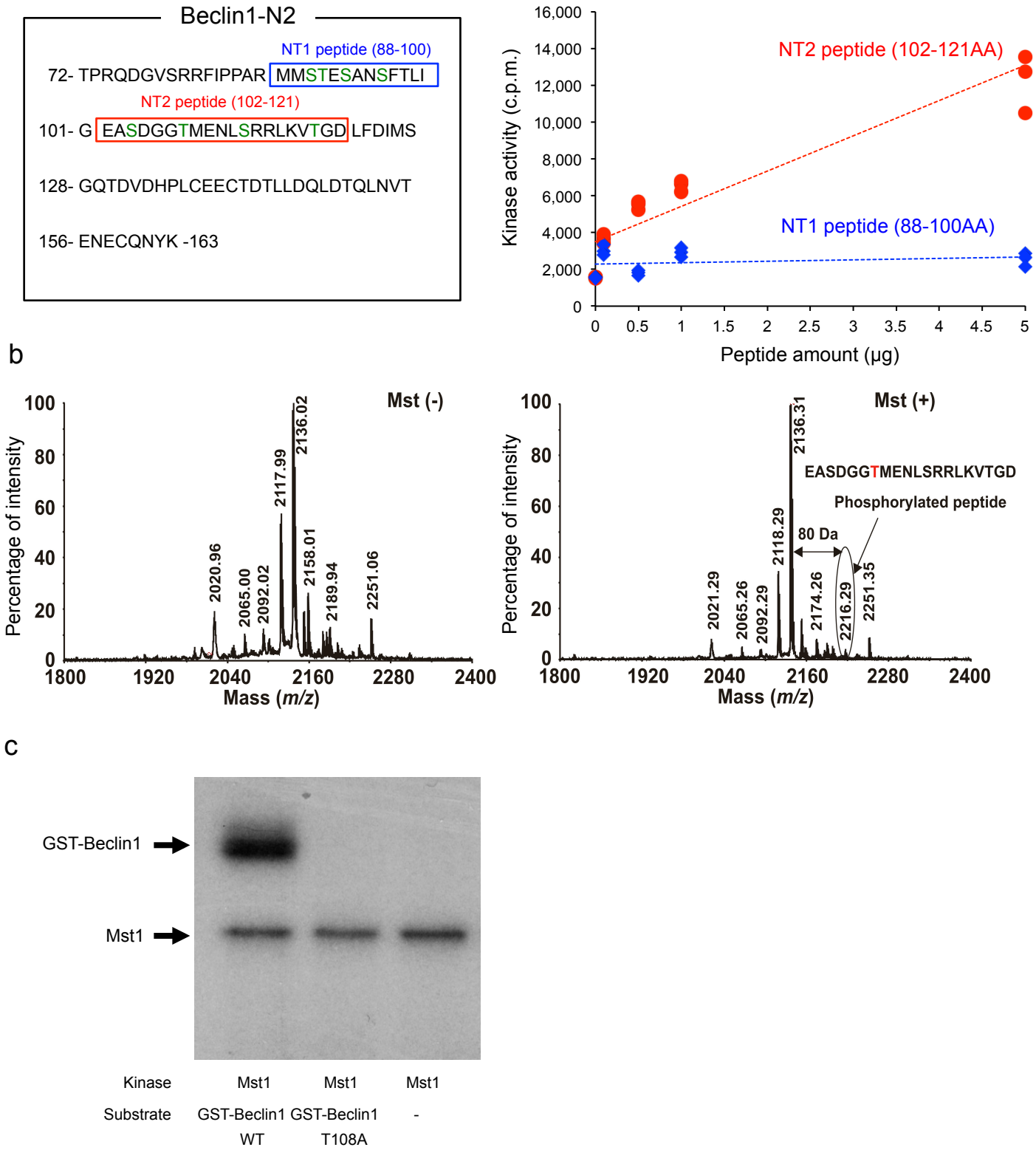

Supplementary Figure 4. Mst1 phosphorylates the BH3 domain of Beclin1 at Thr^{108}.
a, The indicated recombinant partial peptides of Beclin1 were incubated with recombinant Mst1 in the presence of ^{32}P-labeled ATP for *in vitro* kinase assays. Kinase activity of Mst1 was measured in an LSC (n = 3 in each group). **b,** The MS spectra of the Beclin1-NT2 peptide [102-121]. The peptide treated with Mst1 contained a phosphorylated Thr^{108}. **c,** *In vitro* kinase assays were carried out by incubating recombinant GST-Beclin1-WT or GST-Beclin1-T108A proteins with recombinant Mst1 in the presence of ^{32}P-labeled ATP. Reactions were analyzed by SDS-PAGE followed by autoradiography. A representative image of autoradiography is shown. Results represent means from 3 independent experiments.

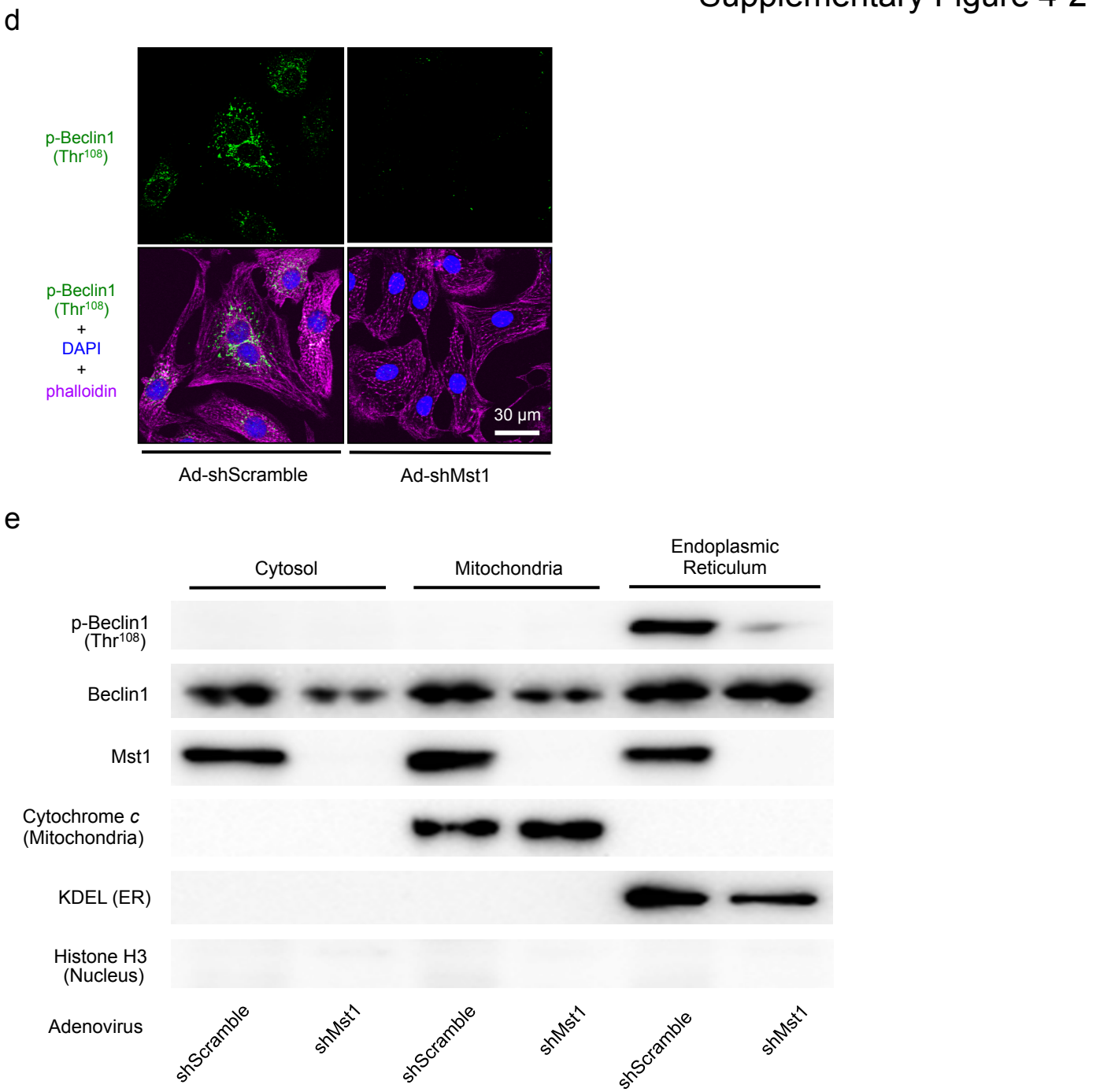

Supplementary Figure 4. (continued)
d, Representative immunofluorescent images of staining with phospho-Beclin1 (Thr^{108}) antibody labeled with Alexa Fluor®488 (green), DAPI (blue), and Alexa Fluor® 555 phalloidin (violet) in Ad-shScramble and Ad-shMst1-transduced CMs are shown. Results represent means from 4 independent experiments. **e,** Cytosolic, endoplasmic reticulum, and mitochondrial membrane fractions were prepared from Ad-shScramble- and Ad-shMst1-transduced CMs. Immunoblot analyses were conducted with phospho-Beclin1 (Thr^{108}) antibody and Beclin1 antibody. The purity of the microsomal fraction was confirmed by the lack of histone H3 or cytochrome *c* staining. The purity of the cytosolic fraction was confirmed by the lack of KDEL. Representative immunoblot images are shown. Results represent means from 3 independent experiments.

Supplementary Figure 5-1

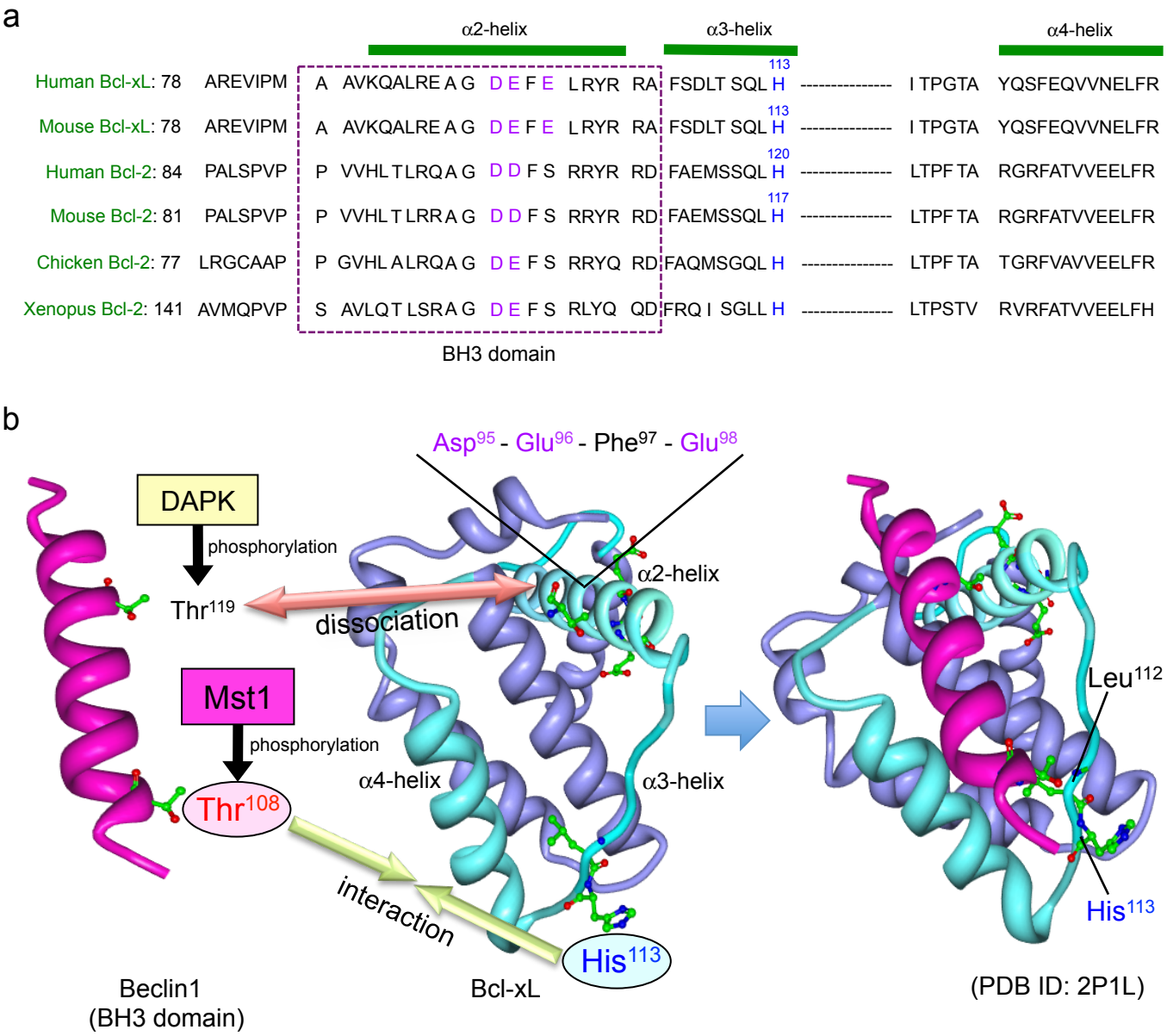

Supplementary Figure 5. Mst1-induced phosphorylation induces homodimerization of Beclin1.
a, Sequence comparison of α2- through α4-helices among Bcl-2 family members. Purple characters indicate acidic amino acids, and blue characters indicate basic amino acids. **b,** A hypothetical model of the interaction between the BH3 domain of human Beclin1 and human Bcl-xL. Mst1-phosphorylated Thr^{108} of human Beclin1 may interact with His^{113} of human Bcl-xL.

Supplementary Figure 5-2

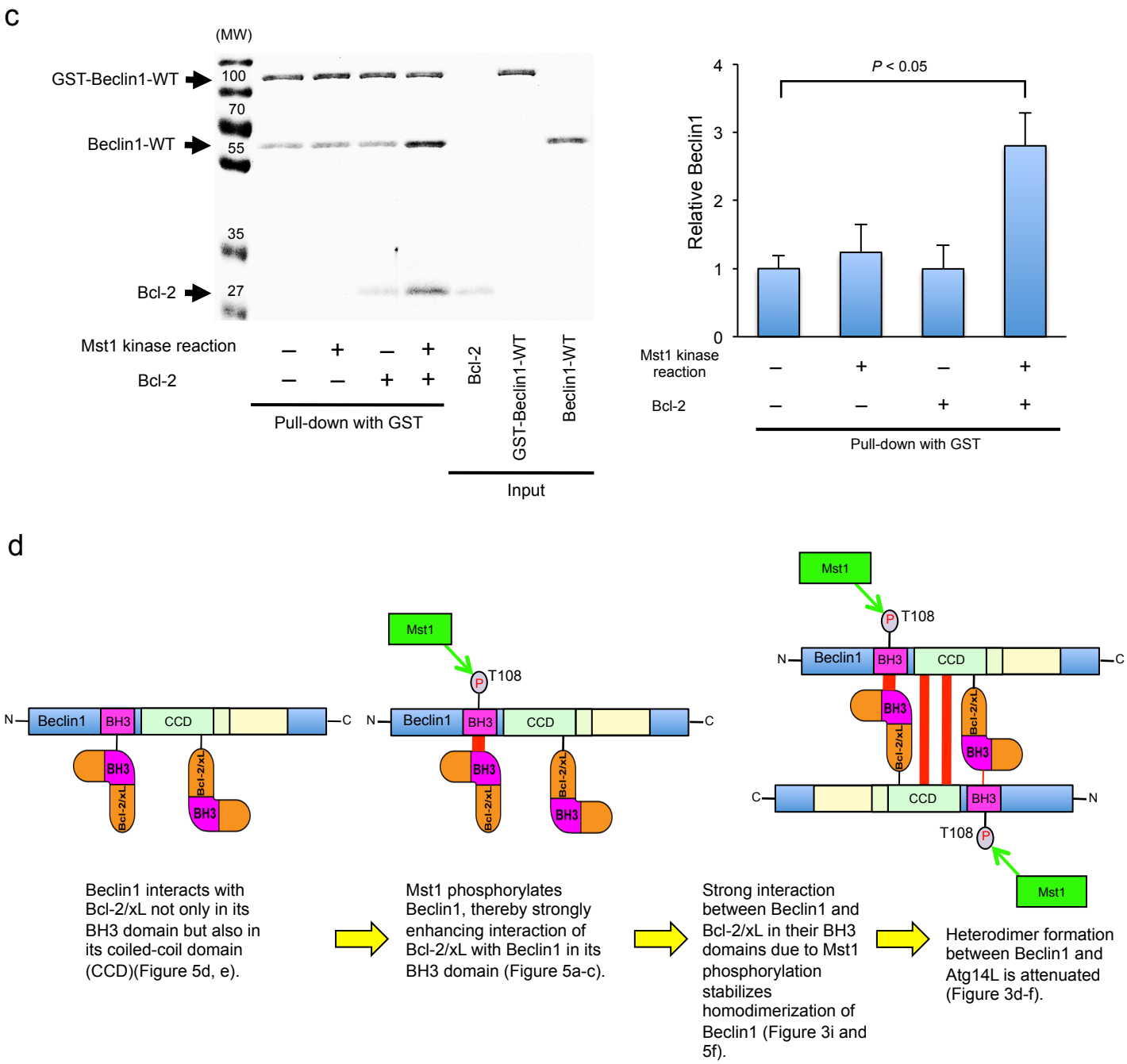

Supplementary Figure 5. (continued)
c, Pull-down assays after kinase reaction. GST-Beclin1-WT incubated with Bcl-2-WT protein after kinase reaction with or without Mst1 was UV-crosslinked by sulfo-NHS-SS-diazirine, and then incubated with non-tagged recombinant Beclin1-WT protein. A representative image is shown. Results represent means from 3 independent experiments. **d,** Schematic model of Mst1, Beclin1, and Bcl-2/Bcl-xL interactions in the regulation of Beclin1 homodimerization and autophagy.

Supplementary Figure 6-1

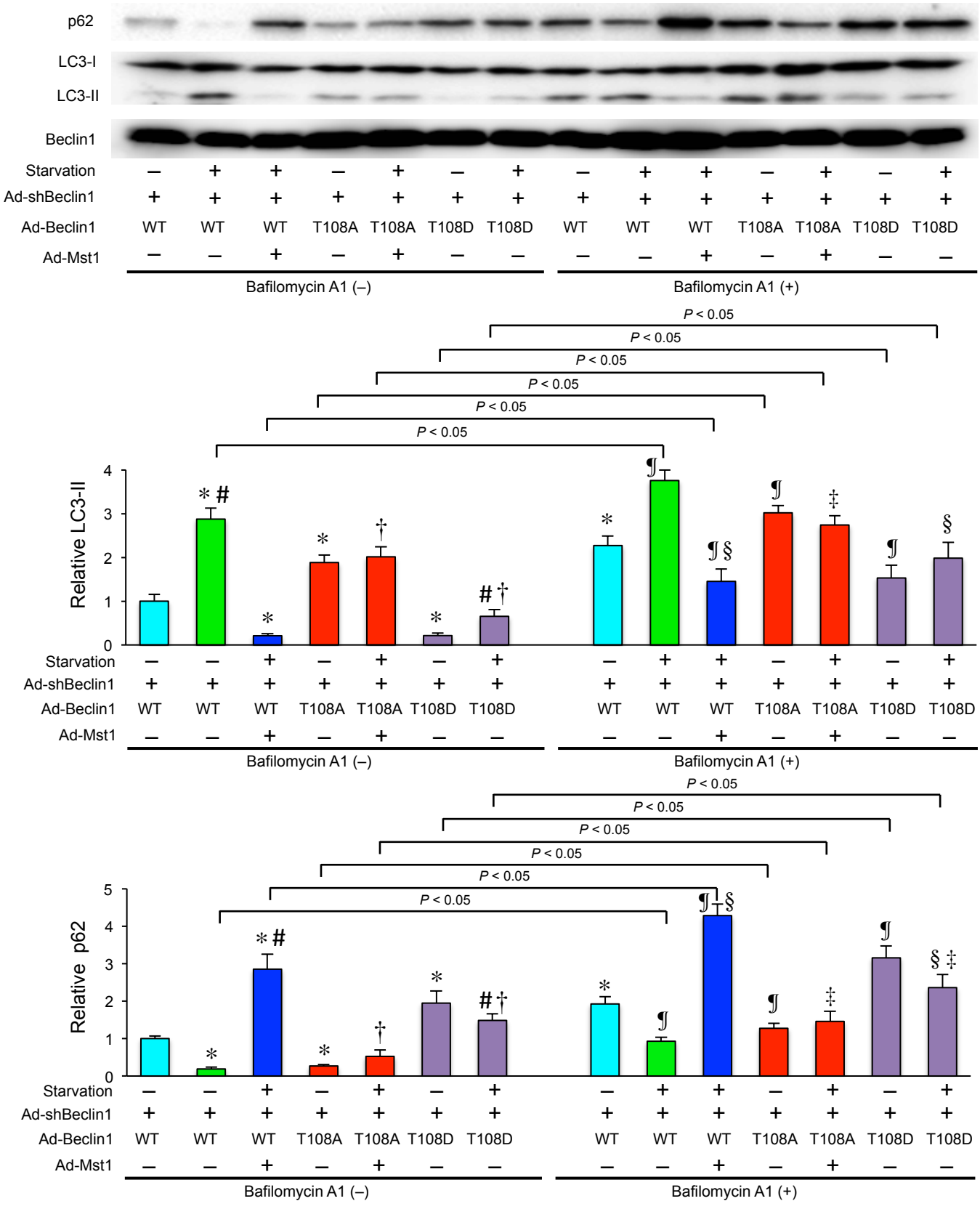

Supplementary Figure 6. Mst1-induced phosphorylation of Beclin1 not only inhibits autophagy but also induces apoptosis by sequestering Bcl-2 from Bax.

a, Cardiomyocytes transduced with Ad-shBeclin1 and Ad-Mst1, Ad-Beclin1-WT, Ad-Beclin1-T108A or Ad-Beclin1-T108D were treated with a glucose-free medium for 4 hours. Some experiments were conducted in the presence of bafilomycin A1. *Upper:* Representative immunoblot pictures are shown. *Middle and Lower:* Quantitative analyses of the p62/SQSTM1 protein amount and the LC3-II amount are shown ($n = 3$ in each group). Data are reported as mean ± SEM. * $P < 0.05$ vs Ad-3xFlag-Beclin1-WT/Starvation(–)/Bafilomycin A1(–); # $P < 0.05$ vs Ad-3xFlag-Beclin1-WT/Starvation(+)/Bafilomycin A1(–); † $P < 0.05$ vs Ad-3xFlag-Beclin1-WT+Ad-Mst1/Starvation(+)/Bafilomycin A1(–); ¶ $P < 0.05$ vs Ad-3xFlag-Beclin1-WT/Starvation(–)/Bafilomycin A1(+); § $P < 0.05$ vs Ad-3xFlag-Beclin1-WT/Starvation(+)/Bafilomycin A1(+) ; ‡ $P < 0.05$ vs Ad-3xFlag-Beclin1-WT+Ad-Mst1/Starvation(+)/Bafilomycin A1(+).

b

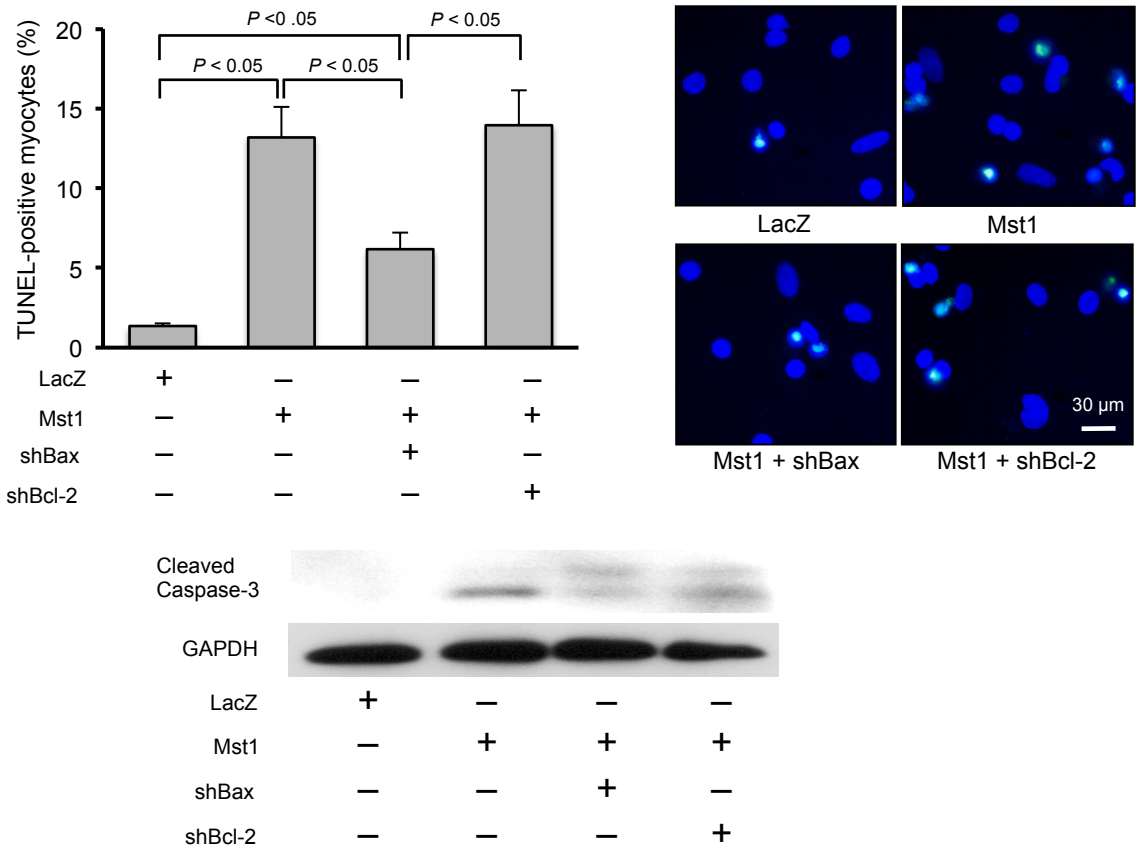

c

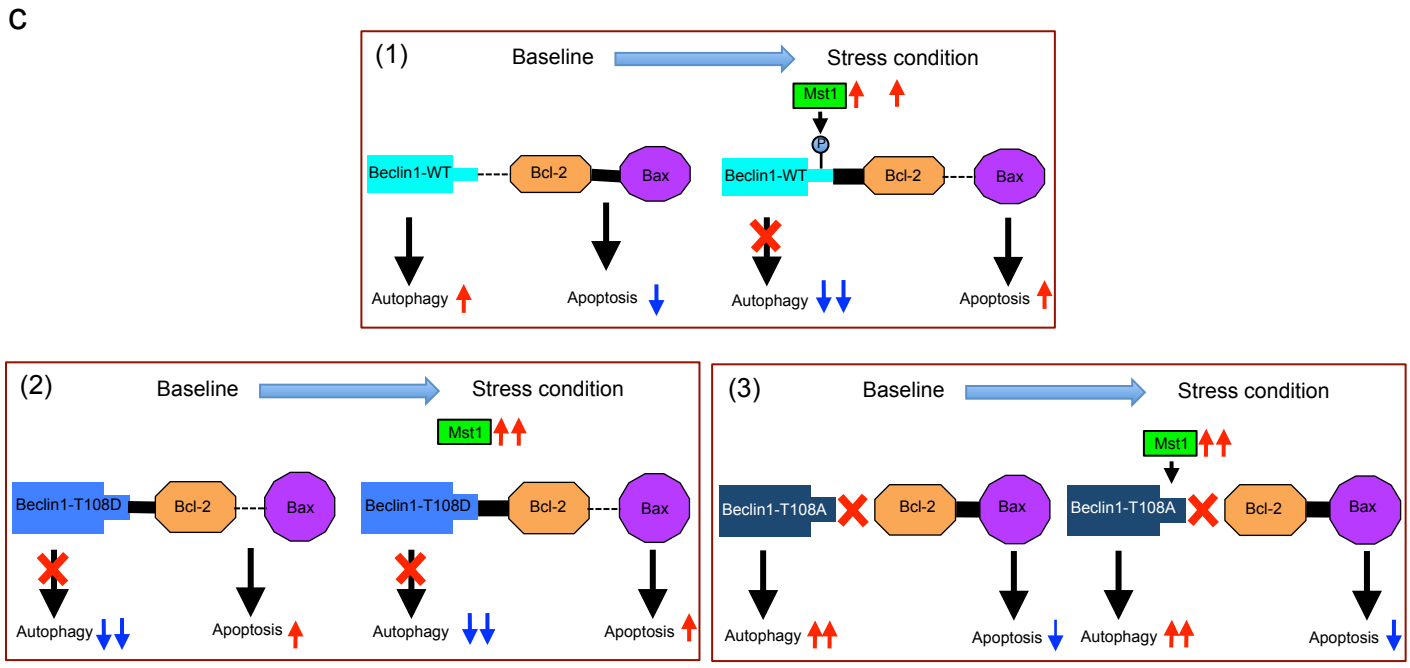

Supplementary Figure 6. (continued)

b, Cardiomyocytes were transduced with or without Ad-Mst1 either in the absence or presence of Ad-sh-Bax or Ad-sh-Bcl-2. *Upper left:* Quantitative analysis of the number of TUNEL-positive myocytes is shown (n = 3 in each group). Data are reported as mean ± SEM. *Upper right:* Representative images of TUNEL-positive myocytes are shown. *Lower:* Immunoblot analysis of cardiomyocytes with cleaved caspase-3 antibody. Representative immunoblot images are shown. Results represent means from 3 independent experiments. **c,** Schematic model of Mst1, Beclin1, Bcl-2 and Bax interactions in the regulation of crosstalk between apoptosis and autophagy. (1) During stress conditions, activated Mst1 phosphorylates Beclin1, thereby inducing apoptosis by promoting sequestration of Bcl-2 from Bax, as well as inhibiting autophagy by promoting interaction of Beclin1 with Bcl-2. (2) The Beclin1-T108D phospho-mimetic mutant not only increased interaction between Bcl-2 and Beclin1, but also attenuated the interaction between Bcl-2 and Bax and increased apoptosis. (3) The Beclin1-T108A phospho-resistant mutant not only decreased interaction between Bcl-2 and Beclin1 but also enhanced the interaction between Bcl-2 and Bax and decreased apoptosis, even though the expression of Mst1 was increased.

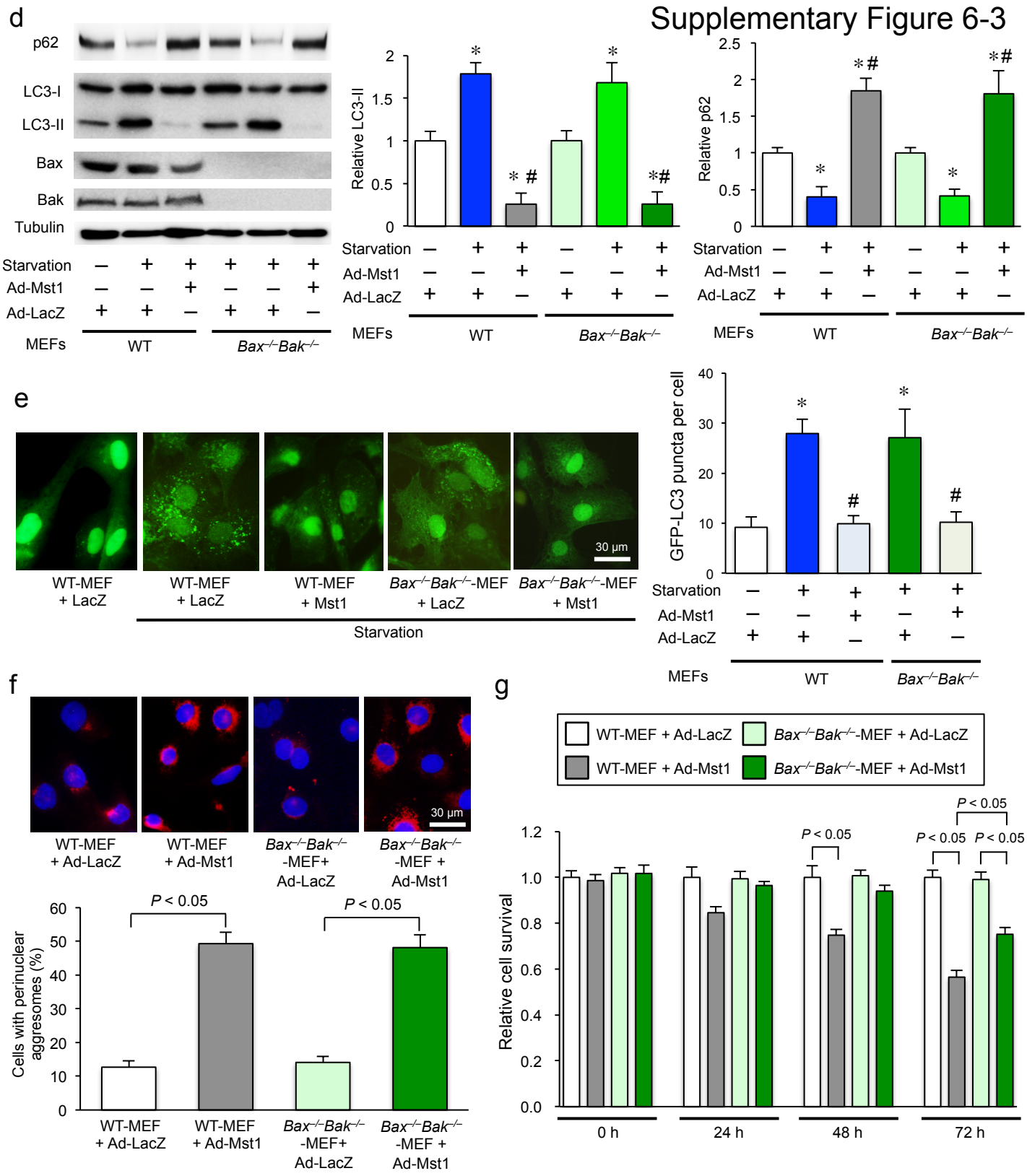

Supplementary Figure 6. (continued)

d, *Bax*$^{-/-}$*Bak*$^{-/-}$-MEFs or WT-MEFs with Ad-Mst1 or Ad-LacZ transduction were treated with a glucose-free medium for 2 hours. *Left:* Representative immunoblot pictures are shown. *Middle and Right:* Quantitative analyses of the LC3-II and p62/SQSTM1 protein amounts are shown ($n = 3$ in each group). Data are reported as mean ± SEM. * $P < 0.05$ vs WT-MEFs/GD(–); # $P < 0.05$ vs WT-MEFs/GD(+). **e,** *Bax*$^{-/-}$*Bak*$^{-/-}$-MEFs or WT-MEFs with Ad-Mst1 or Ad-LacZ transduction were transduced with Ad-GFP-LC3. *Left:* Representative images of GFP-LC3 puncta are shown. *Right:* Quantitative analysis of the number of GFP-LC3 puncta is shown ($n = 3$ in each group). Data are reported as mean ± SEM. * $P < 0.05$ vs WT-MEFs/GD(–); # $P < 0.05$ vs WT-MEFs/GD(+). **f,** *Upper:* Representative immunofluorescent images of staining with ProteoStat® aggresome detection reagent (red) and DAPI (blue) in Ad-LacZ-transduced and Ad-Mst1-transduced *Bax*$^{-/-}$*Bak*$^{-/-}$-MEFs or WT-MEFs after 72 hours are shown. *Lower:* The number of cells with aggresomes in MEFs was counted ($n = 6$ in each group). Data are reported as mean ± SEM. **g,** Cell viability was evaluated in *Bax*$^{-/-}$*Bak*$^{-/-}$-MEFs or WT-MEFs after transduction with Ad-Mst1 or Ad-LacZ ($n = 12$ in each group). Data are reported as mean ± SEM.

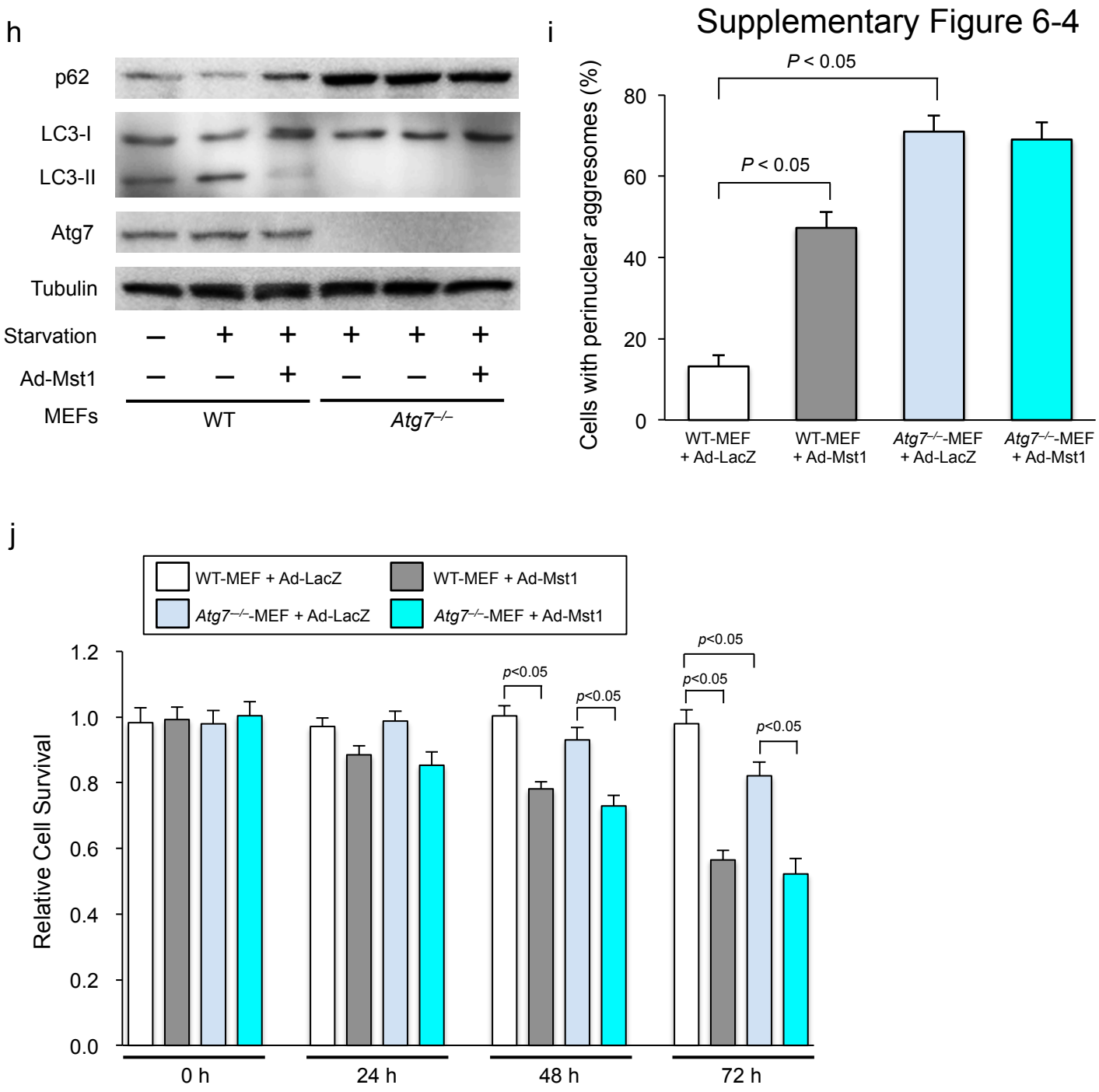

Supplementary Figure 6. (continued)
h, *Atg7*$^{-/-}$-MEFs or WT-MEFs with Ad-Mst1 or Ad-LacZ transduction were treated with a glucose-free medium for 2 hours. Representative immunoblot pictures are shown. Results represent means from 3 independent experiments. **i,** The number of cells with aggresomes in Ad-LacZ-transduced and Ad-Mst1-transduced *Atg7*$^{-/-}$-MEFs or WT-MEFs after 72 hours was counted ($n = 6$ in each group). Data are reported as mean ± SEM. **j,** Cell viability was evaluated in *Atg7*$^{-/-}$-MEFs or WT-MEFs after transduction with Ad-Mst1 or Ad-LacZ ($n = 12$ in each group). Data are reported as mean ± SEM.

k

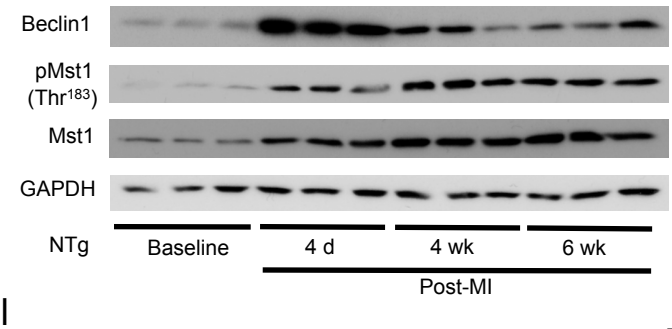

l

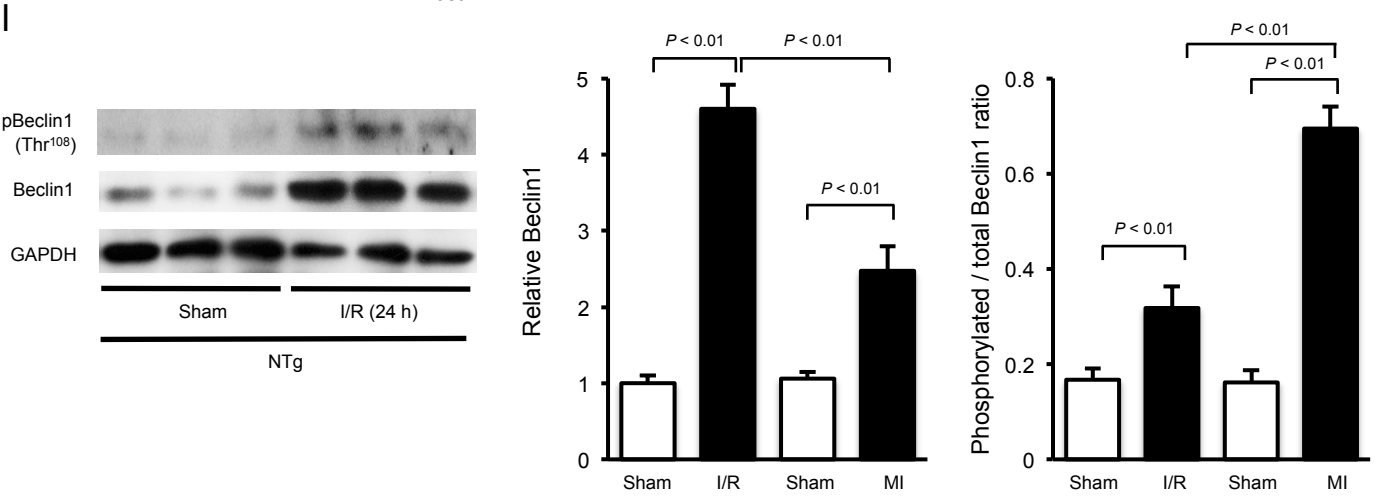

m

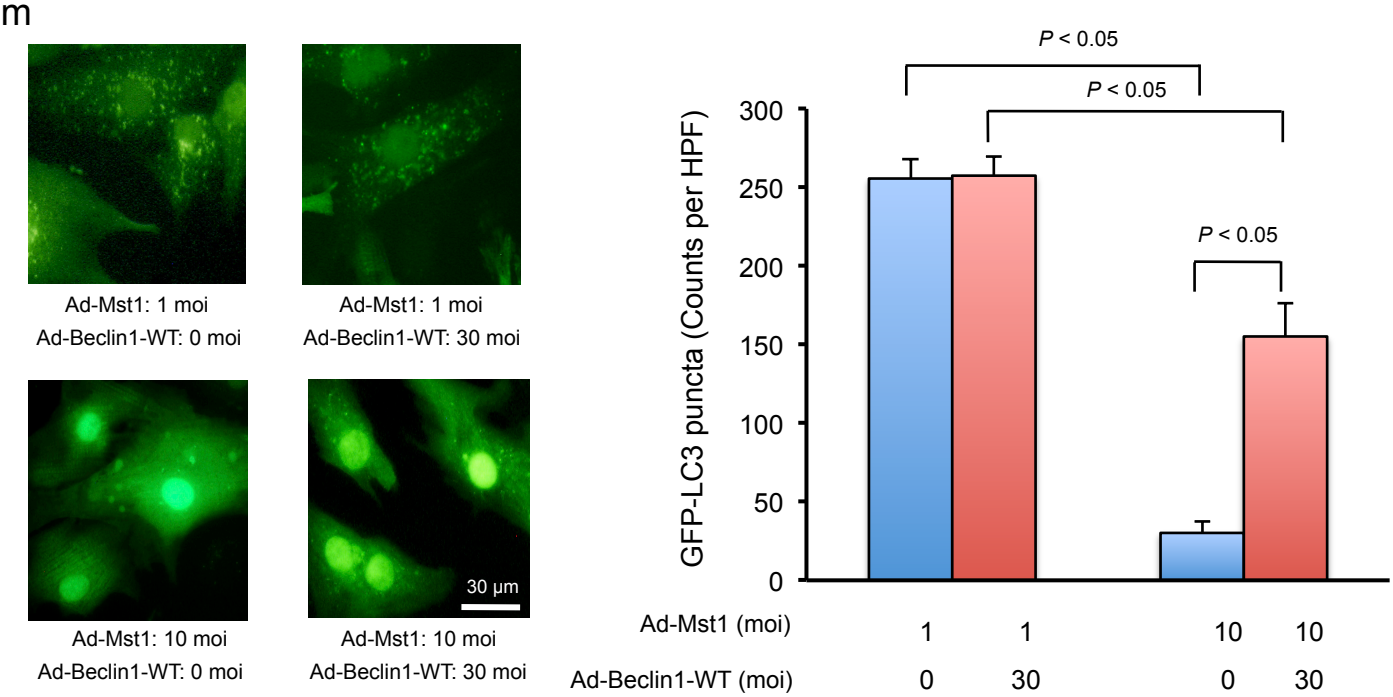

Supplementary Figure 6. (Continued)
k, The changes in total Beclin1, phospho-Mst1 (Thr^{183}), and total Mst1 levels over time in NTg mouse hearts after coronary artery ligation were evaluated by immunoblot analyses. Representative images are shown. Results represent means from 3 independent experiments. **l,** NTg mice were subjected to 20 min of ischemia, followed by reperfusion for 24 h. *Left:* The amounts of Beclin1 and phosphorylated Beclin1(Thr^{108}) in the heart were determined by immunoblotting. *Middle:* The results of the quantitative analysis of Beclin1 after I/R and chronic MI (shown in Fig. 6e). *Right:* Quantitative analysis of the phosphorylated Beclin1 / total Beclin1 after I/R and chronic MI (shown in Fig. 6e). Data are reported as mean ± SEM. **m,** CMs transduced with Ad-Mst1 and/or Ad-Beclin1-WT 24 h after Ad-GFP-LC3 transduction were treated with a glucose-free medium for 4 h. *Upper:* Representative images of GFP-LC3 puncta are shown. *Lower:* Quantitative analysis of the number of GFP-LC3 puncta is shown (n = 6 in each group). Data are reported as mean ± SEM.

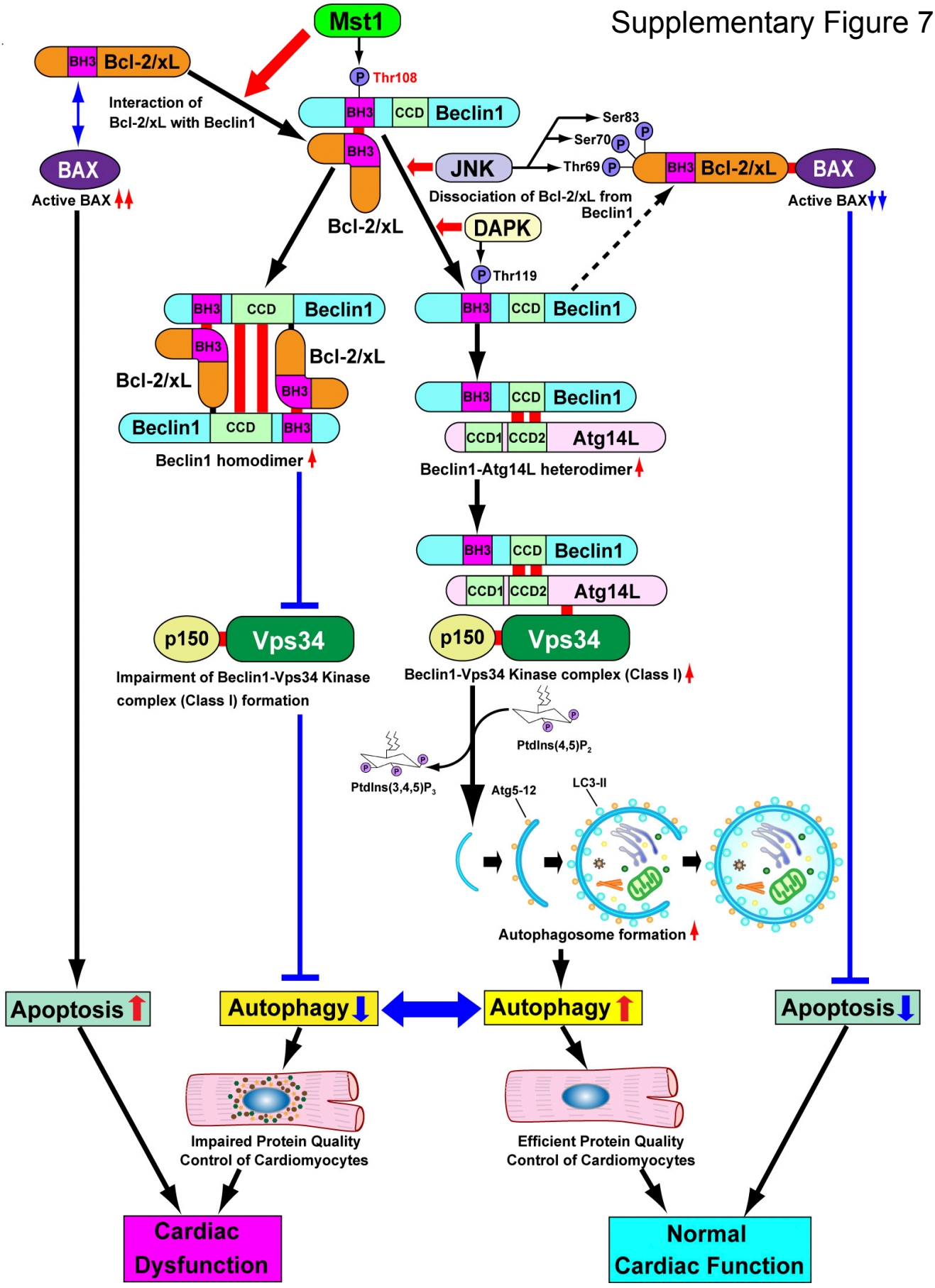

Supplementary Figure 7. Schematic model of Mst1, Beclin1, and Bcl-2/xL interactions in the regulation of autophagy in the heart.

Mst1 phosphorylates the BH3 domain of Beclin1 at Thr^{108}, leading to enhancement of Beclin1-Bcl-2/xL interaction, Beclin1 homodimerization, and suppression of Vps34 kinase activity, thereby inhibiting autophagosome formation. Activation of Mst1 by stress suppresses autophagy below physiological levels and inhibits protein quality control, which in turn may contribute to cardiac dysfunction. Furthermore, Mst1-mediated interaction between Beclin1 and Bcl-2 family proteins also induces apoptosis by sequestering Bcl-2 family proteins from Bax.

Supplementary Table 1

A list of the characteristics of the heart transplant recipients and donors enrolled in the experiments of Figure 6f and 6g.

Donors			Recipients			
Case#	Age*	Sex	Case#	Age*	Sex	Diagnosis
1a	25.9	M	1b	53.7	M	Dilated cardiomyopathy
2a	38.1	M	2b	53.5	F	Dilated cardiomyopathy
3a	33.9	M	3b	42.4	M	Dilated cardiomyopathy
4a	45.2	M	4b	26.1	M	Dilated cardiomyopathy
5a	46.3	F	5b	55.4	M	Dilated cardiomyopathy
6a	24.8	M	6b	23.4	M	Dilated cardiomyopathy
∗ Mean ± SEM = 35.7 ± 3.8			∗ Mean ± SEM = 36.8 ± 7.5			